Dalton Transactions

An international journal of inorganic chemistry

Accepted Manuscript

ROYAL SOCIETY OF CHEMISTRY

rsc.li/dalton

View Article Online
DOI: 10.1039/D0DT01665A

Ciprofloxacin conjugated to diphenyltin(IV); A novel formulation with enhanced antimicrobial activity.

M.P. Chrysouli[a], C.N. Banti[a],*, N. Kourkoumelis[b], E.E. Moushi[c], A.J. Tasiopoulos[d], A. Douvalis[e], C. Papachristodoulou[f], A.G. Hatzidimitriou[g], T. Bakas[e], S.K. Hadjikakou[a,h],*

[a] Inorganic and Analytical Chemistry, Department of Chemistry, University of Ioannina, 45110 Ioannina, Greece

[b] Medical Physics Laboratory, Medical School, University of Ioannina, Greece

[c] Department of Life Sciences, The School of Sciences, European University Cyprus, Cyprus

[d] Department of Chemistry, University of Cyprus, 1678 Nicosia, Cyprus

[e] Mössbauer Spectroscopy and Physics of Material Laboratory, Department of Physics, University of Ioannina, Greece

[f] Department of Physics, University of Ioannina, Greece

[g] Department of Chemistry, Aristotle University of Thessaloniki, Greece;

[h] University Research Center of Ioannina (URCI), Institute of Materials Science and Computing, Ioannina, Greece

*All correspondence should be addressed to:

Dr. C.N. Banti (Postdoctoral Fellow); email: cbanti@uoi.gr

Dr. S.K. Hadjikakou (Professor); e-mail: shadjika@uoi.gr; tel. x30-26510-08374, x30-26510-08362

View Article Online
DOI: 10.1039/D0DT01665A

Abstract

The metalloantibiotic of formula $Ph_2Sn(CIP)_2$ (**CIPTIN)** (**HCIP**= ciprofloxacin) was synthesized by reacting ciprofloxacin hydrocloride (**HCIP·HCl**) (an antibiotic in clinical use) with the diphenyltin dichloride (Ph_2SnCl_2 **DPTD**). The complex was characterized in solid state by melting point, FT-IR, X-ray Powder Diffraction (XRPD) analysis, ^{119}Sn Mössbauer spectroscopy, X-ray Fluorescence (XRF) spectroscopy, Thermogravimetry/Differential Thermal Analysis (TG-DTA) and in solution by UV-Vis, ^{1}H-NMR spectroscopic techniques and Electrospray Ionisation Mass Spectrometry (ESI-MS). The crystal structure of **CIPTIN** and its processor **HCIP** were also determined by X-ray crystallography.

The antibacterial activity of **CIPTIN**, **HCIP·HCl**, **HCIP** and **DPTD** was evaluated against the bacterial species *Pseudomonas aeruginosa* (*P. aeruginosa*), *Escherichia coli* (*E. coli*), *Staphylococcus aureus* (*S. aureus*) and *Staphylococcus epidermidis* (*S. epidermidis*), by the means of Minimum Inhibitory Concentration (MIC), Minimum Bactericidal Concentration (MBC) and Inhibition Zones (IZs). **CIPTIN** shows lower MIC values than those of **HCIP·HCl** (up to 4.2-folds), **HCIP** (up to 2.7-folds) or **DPTD** (>135-folds), towards the tested microbes. **CIPTIN** is classified to bactericidal agents according to MBC/MIC values. The developing IZs are 40.8±1.5, 34.0±0.8, 36.0±1.1 and 42.7±0.8 mm, respectively which classify the microbe's *P. aeruginosa*, *E. coli*, *S. aureus* and *S. epidermidis* to susceptible ones to **CIPTIN**. These IZ's are greater to the corresponding ones of the **HCIP·HCl** by 1.1 to 1.5-folds against both Gram negative and positive bacteria tested. **CIPTIN** eradicates the biofilm of *P. aeruginosa* and *S. aureus* more efficiently than **HCIP·HCl** and **HCIP**. The *in vitro* toxicity and genotoxicity of **CIPTIN** were tested against human skin keratinocyte cells (HaCaT) (IC_{50}= 2.33 μM). **CIPTIN** exhibits 2 to 9-folds lower MIC values against than its IC_{50} against HaCaT, while its genotoxic effect determined by micronucleus assay is equivalent to the corresponding ones of **HCIP·HCl** or **HCIP**.

Keywords: Bioinorganic Chemistry; Organotin(IV) Compounds; Crystal Structure; Antibacterial Studies; Ciprofloxacin

Introduction

View Article Online
DOI: 10.1039/D0DT01665A

Ciprofloxacin, a second-generation fluoroquinolone, is effective against both *Gram*-positive and *Gram*-negative pathogenic bacteria [1]. It exhibits good bioavailability or tissue permeability, low incidence of toxic effects and bacteriostatic activity [2]. Generally, the bacteriocidal agents are preferred than bacteriostatic ones, against infections, since they limit the development of resistance towards bacteria [3]. However, microbes such as *P. aeruginosa*, *E. coli*, *S. aureus* and *S. epidermidis* are reported to have developed resistance towards ciprofloxacin [4]. Hence efforts were made in recent years to modify ciprofloxacin with metal ions, in order to increase its antibacterial activity against resistant strains [5-8].

The conjugation of metals with drugs (CoMeDs), is a new research area being investigated for discovery of new synergistic therapeutic modalities. The term "conjugation" is used for polymeric drug formulations, to emphasize the synergistic effect of a metal with a drug [9-10]. CoMeDs combine metals with specific classes of drugs aiming to create new agents possessing altogether new properties than the drugs from which they were prepared [9-10]. From this point of view, organotin(IV) compounds which contain active drugs as ligands are expected to exhibit enhance effectiveness due to the synergy which is developing between the $R_nSn(IV)$ (R= alkyl or aryl group; n=1 to 3) moiety and the drug. Besides, organotin compounds are commercially used as agricultural biocides [11-12]. Recently, Pokharia et.al have shown that triorganotin(IV) complexes of ciprofloxacin ($R_3Sn(CIP)$ (R= Me-, Cy-)) exhibit better antibacterial effect than free ciprofloxacin against *E. faecalis*, *S. aureus*, *K. pneumoniae*, *E. coli*, *P. aeruginosa*, and *P. mirabilis* [13].

With the aim to develop new antimicrobial agents with enhanced activity capable of overcoming bacterial resistance [9,10,14-17], the metalloantibiotic of ciprofloxacin (**HCIP,** (Scheme 1)), having the formula $Ph_2Sn(CIP)_2$ (**CIPTIN)** was synthesized, characterized and evaluated against bacterial strains *P. aeruginosa*, *E. coli*, *S. aureus* and *S. epidermidis*. Moreover, the combination of an antibiotic, ciprofloxacin, which possesses pharmacological significance and a

metal with known biological activity, tin(IV), are expected to throw light on principles that govern the synergy between metals and drugs in these metallodrugs.

View Article Online
DOI: 10.1039/D0DT01665A

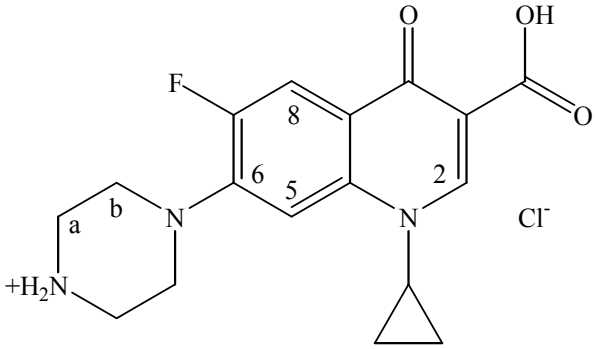

Scheme 1. The used ligand hydrocloride ciprofloxacin

Results and discussion

General aspects: A solution of **HCIP·HCl** in water was initially treated with an excess of KOH in 1:1.5 molar ratio to form **KCIP**. A solution of **DPTD** (Ph_2SnCl_2, diphenyltin dichloride) in MeOH (1:2 metal to **KCIP**) was added to the previous one under continues stirring for 30 min, (Scheme 2) and the suspension was filtered off.

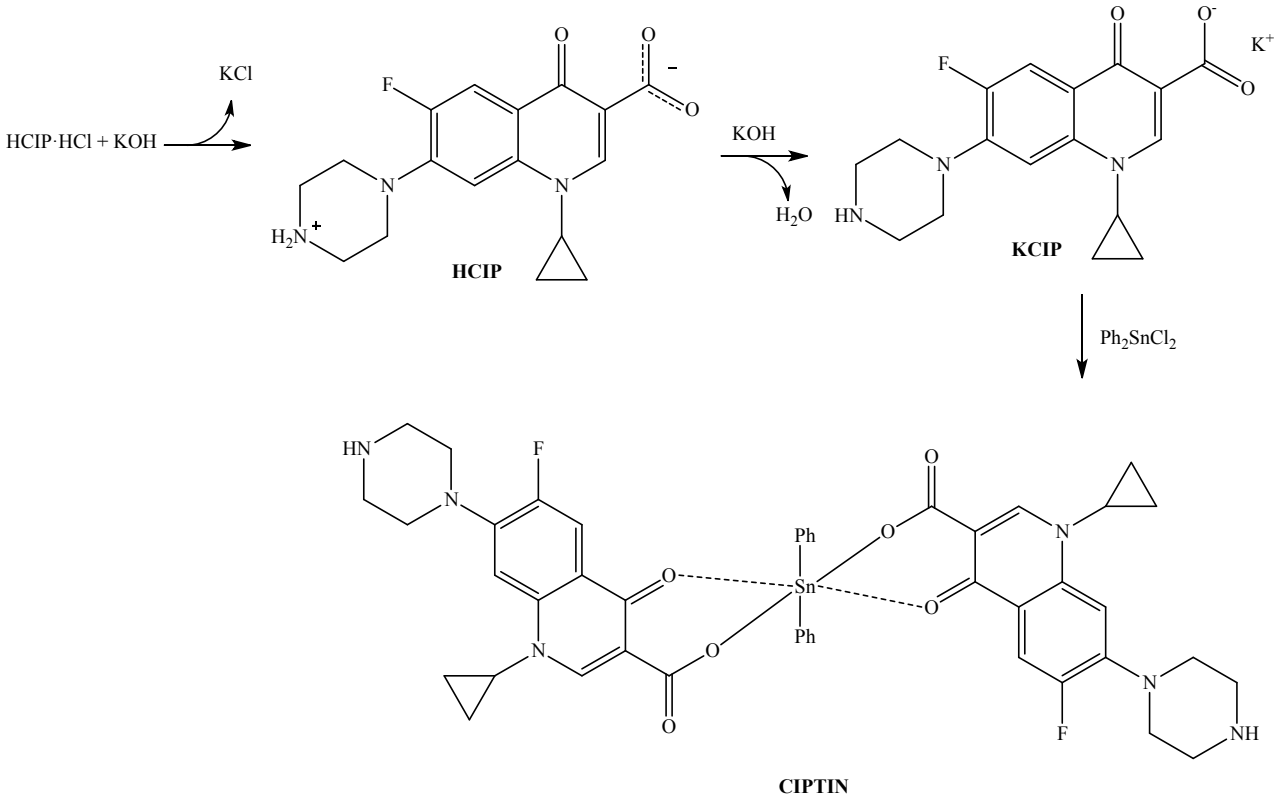

Scheme 2. Preparation reaction of **CIPTIN**

View Article Online
DOI: 10.1039/D0DT01665A

Crystals of **CIPTIN** were grown by slow evaporation of ddH_2O/MeOH solution. Besides, crystals of the **HCIP** were isolated from the filtrate of the intermediate solution (Scheme 2). **CIPTIN** is stable when it is stored at ambient condition and it is soluble in MeOH, CH_2Cl_2, DMSO and acetone.

Solid state studies

*Crystal and molecular structure of **CIPTIN** and **HCIP**:* Here we report the crystal structures of the zwitterionic form of **HCIP** (anhydrous) and that of **CIPTIN** using single crystal X-Ray crystallography for the first time. Unit cell parameters (only) of anhydrous **HCIP** was determined earlier from powder X-Ray diffraction data by Fabbiani et al. [18]. The reported unit cell parameters reveal **HCIP** crystallizes in P-1 space group with a = 7.9606(2), b = 8.5798(2) and c = 10.7739(3) Å, α = 87.868(4), β = 87.868(4), γ = 88.212(4)°, V = 732.43(4) Å^3 [18]. In our study we found HCIP (anhydrous) crystallizes in P-1 space group with almost identical unit cell parameters: a = 7.8945(7), b = 8.5010(8) and c = 10.7522(9) Å and α= 87.440(7), β= 84.496(7) γ= 88.912(7)°, V= 717.47 Å^3. Since synthesis of **CIPTIN** requires **HCIP HCl** as starting material, **HCIP** is an intermediate of the methodology for the preparation. For this reason, a complete refinement of the crystal structure of **HCIP** was attempted independently to clarify the route followed. ORTEP diagrams of **CIPTIN** and **HCIP** along with their selected bond distances and angles are shown in Figures 1-2.

Figures 1-2

CIPTIN is a covalent organotin compound. It consists of two ciprofloxacin ligands and one Ph_2Sn(IV) moiety. Ciprofloxacin coordinates to tin(IV) through the anionic oxygen atom of its de-protonated carboxylic group and the oxygen atom of its keto group. Thus, two oxygen atoms from

View Article Online
DOI: 10.1039/D0DT01665A

each ciprofloxacin and two carbon atoms from the phenyl groups form a distorted octahedral (Oh) arrangement around the Sn(IV) ion. The equatorial plane of the octahedron around the Sn(IV) is constituted by two keto oxygen atoms (O3, O3a) and two carbons of phenyl groups (O3-Sn1-O3a= 80.96(11)^{o}, O3-Sn1-C18a= 166.12(15) ^{o}). The axial positions are occupied by the two carboxylic oxygen atoms (O1 and O1a) (O1-Sn1-O1a= 155.64(11)^{o}). The final arrangement of the ligands in **CIPTIN** lead to the Δ-*cis*-[$Ph_2Sn(CIP)_2$] stereoisomer (Figure 1B). Only the Δ-*cis*-[$Ph_2Sn(CIP)_2$] isomer has been isolated in the crystal lattice indicating stereo-selectivity of the preparation reaction (Figure 1B).

The two C-O bond distances of the carboxylic group (O1-C6= 1.298(5) and O2-C6= 1.216(5) Å) are almost equivalent, in **CIPTIN**, confirming the deprotonation which it undergoes. The O1-C6 bind is slightly longer than the corresponding O2-C6 one due to the donation of O1 atom towards Sn(IV). The C-O bond length of keto group (O3-C2= 1.284(5) Å) suggesting the retention of the double nature of this bond.

The Sn-O bond distances (Sn1-O1= 2.135(3) and Sn1-O3= 2.158(3) Å) are in accordance to the corresponding ones found previously in [(*n*-Bu-)$_2$Sn(nap)$_2$] (napH= naproxen) (Sn1-O1= 2.136(7) and Sn1-O2= 2.506(6) Å) [19], in [$Me_2Sn(salH)_2$] ($salH_2$= salicylic acid)) (Sn1-O171= 2.1069(18), Sn1-O271= 2.1087(15), Sn1-O172= 2.5145(15) and Sn1-O272= 2.5773(15) Å) [20] and in [(*n*-Bu)$_2$Sn(salH)$_2$] (Sn1-O172= 2.121(3), Sn1-O272= 2.105(4), Sn1-O171= 2.565(4) and Sn1-O271= 2.632(4) Å) [20]. However, in the cases of [(*n*-Bu-)$_2$Sn(nap)$_2$], [$Me_2Sn(salH)_2$] and [(*n*-Bu)$_2$Sn(salH)$_2$] the ligands chelate to Sn(IV), through their carboxylic groups.

Strong hydrogen bonding interactions N3[H3]···O2= 2.733(6) Å lead to 2D layers (Figure 3). The layers are consisted of squares which are formed by four **CIPTIN** molecules (Sn···Sn=13.969 Å and Sn-Sn-Sn= 87.03^{o}).

Figure 3

View Article Online
DOI: 10.1039/D0DT01665A

The two C-O bond distances of the carboxylic group in anhydrous **HCIP** (O1-C14= 1.247(3) and O2-C14 (1.266(3) Å) are equivalent suggesting its de-protonation (Figure 2). The corresponding C1-O1, C1-O2 bond lengths of the HCIP hexahydrate (**HCIP·6H$_2$O**) are 1.259(2) and 1.255(2) Å respectively [8]. Moreover, the O1-C14-O2 angle is 125.3(2)°. This is in accordance to the corresponding bond angle found in **HCIP·6H$_2$O** (125.11(12)°) [8]. The N3-C11 and N3-C12 bond distances, on the other hand, are 1.481(3) and 1.485(3) Å, respectively, suggesting single N-C bonds (Figure 2). This is further supported by the C11-N3-C12 bond angle of 109.0(2)°, which is close to the ideal 108° 28' of sp^3 hybrid. Given that two hydrogen atoms are bind to this nitrogen, a positive charge is concluded for the ([-NH$_2$-])$^+$ group. Therefore, the charge distribution of the zwitterionic anhydrous **HCIP** is shown in Scheme 2.

Hydrogen bonds N3[H3]···O2= 2.623(3) Å and N3[H3]···O1= 2.882(3) Å lead to 1D ribbon assembly (Figure 2B).

Vibrational spectroscopy: The characteristic vibration bands of the free ligand (**HCIP·HCl)** at 1710 cm^{-1}, 1620 cm^{-1} and 1385 cm^{-1} are assigned to the C=O, ν_{asym}(COO) and ν_{sym}(COO) vibrations, respectively (Figure S1). The absence of the vibration band at 1710 cm^{-1} in the spectrum of **CIPTIN**, suggests the coordination of the ligand through the oxygen atom of the keto C=O group (Figure S1). The ν_{asym}(COO) and ν_{sym}(COO) vibration bands are shifted at 1622 cm^{-1} and at 1381 cm^{-1}, respectively in the spectrum of **CIPTIN**. The presence of C=N band of **CIPTIN** at 1272 cm^{-1}, suggests that this N atom is not involving in the coordination sphere of the metal. The absence of (O-H) vibration at 3520 cm^{-1} in **CIPTIN** spectrum indicates the deprotonation of the carboxyl group. Therefore ciprofloxacin is coordinated to the tin metal ion via the keto and the carboxyl oxygen atom (Figure S1).

X-ray Powder Diffraction (XRPD) analysis: The XRPD spectrum of the powder of **CIPTIN** is identical to the simulated one which is derived by using single crystal XRD data (Figure S2). This

indicates that the formula of the molecular structure of **CIPTIN** remains unchanged throughout the sample.

View Article Online
DOI: 10.1039/D0DT01665A

^{119}Sn Mössbauer spectroscopy: ^{119}Sn Mössbauer spectrum at 77 K of **CIPTIN** is shown in Figure 4. The spectrum of **CIPTIN**, consists of one asymmetric Lorentzian doublet. The occurrence of one Lorentzian double, indicates either the existence of one type of Sn atom in **CIPTIN** or one structural isomer [11,21-22]. The value of the Isomer Shift (I.S.) of **CIPTIN** is +0.804 mm×s^{-1} which corresponds to the (4+) oxidation state [11,21-22]. The I.S. for $R_2Sn(IV)$ species lie between +0.737 to +1.777 mm×s^{-1} [11,21-22]. The quadrupole splitting parameter (ΔEq) value is 2.242 mm×s^{-1}. Therefore, cis-octahedral geometry should be concluded for tin(IV) ion in the case of **CIPTIN**, since ΔEq value lies between 1.3-2.5 mm×s^{-1} [11,21-22]. This value indicates an octahedral geometry with *cis*-$R_2Sn(IV)$ (R= alkyl), around the tin atom of **CIPTIN** in accordance to X-ray structure.

Figure 4

X-ray Fluorescence (XRF) spectroscopy: The content of **CIPTIN** in Sn is 15.5 ± 2.3% wt, while the calculated for $C_{46}H_{44}F_2N_6O_6Sn$ is 12.75 %.

Thermal analysis: The TG-DTA analysis of **CIPTIN** shows decomposition within 6 steps (112.6-617.4 °C) with total mass losses 57.92% (Figure S3). The remaining 42.08% is due to the $[(SnO_2)_2]$ (which corresponds to Sn: 13.68 %; calc for $C_{46}H_{44}F_2N_6O_6Sn$: 12.75 %).

Solution studies

Stability studies: The stability of **CIPTIN** was tested in DMSO and DMSO/water solutions by UV spectroscopy (Figures S4–S5) and ^{1}H-NMR for a period of 96 h (Figure S6). This period was chosen for the stability testing, since the biological experiments require 24 or 48 h of incubation

View Article Online
DOI: 10.1039/D0DT01665A

with **CIPTIN**. No changes were observed between the initial UV or ^{1}H-NMR spectra and the corresponding ones after 96 h, confirming the retention of **CIPTIN** in solution (Figures S4–S6).

^{1}H NMR studies: A broad resonance signal in the ^{1}H-NMR spectrum of **HCIP·HCl** at 9.45 ppm is attributed to H[$N_{piperazine\ ring}$] [8] (Figure S7). This signal is shifted at 8.87 ppm in **CIPTIN**. The resonance signals at 8.68, 7.97-7.92, 7.62-7.59 ppm, in the spectrum of **HCIP·HCl** are assigned to the H[^{2}C], H[^{5}C] and H[^{8}C], respectively (Scheme 1) [8]. These signals are observed at 8.67, 7.95-7.92, 7.79-7.81 ppm in the spectrum of **CIPTIN**. The resonance signals of H[^{a}C], H[^{b}C], cyclopropyl (–CH_2–) in the spectrum of **HCIP·HCl** are appeared at 3.85, 3.47, 1.33-1.19 ppm, respectively [8]. These signals undergo no shift in the case of the **CIPTIN**. The resonance signals of **DPTD** at 8.05-7.80 and 7.42-7.28 ppm are shifted in the spectrum of **CIPTIN** at 7.72-7.58 and 7.31-7.16 ppm, respectively, indicates the coordination of tin to the antibiotic. Moreover, the resonance signal in the spectrum of **CIPTIN**, at 3.16 ppm is attributed to methanol, which was used as a solvent for the synthesis reaction.

Electrospray Ionisation Mass Spectrometry (ESI-MS): In order to confirm the retention of the formula of **CIPTIN** in methanol solution, its ESI-MS spectrum was recorded. The ESI-MS spectrum of **CIPTIN** is dominated by the fragment at m/z 600.0-609.0 which is attributed to the $[Ph_2Sn(CIP)]^{+}$ (calculated for $[C_{29}H_{27}N_3O_3FSn]^{+}$: m/z: 599.1 to 609.1) (Figure S8). The presence of this specie which is derived from **CIPTIN** by cleavage of the one Sn-C(Ph) bond as part of the decomposition pattern of $[Ph_2Sn(CIP)_2\text{-}H^{+}]$, assumes the existence of **CIPTIN** in the solution, initially.

Antimicrobial studies

Minimum inhibitory concentration (MIC): The Gram-negative (*P. aeruginosa* and *E. coli*) and Gram-positive (*S. aureus* and *S. epidermidis*) are among the most concerning pathogens in human

involved in antibiotic resistance [23-24]. The antimicrobial ability of **CIPTIN** was evaluated towards these strains, in terms of MIC values. The MIC is defined as the lowest concentration for the bacterial growth inhibition [8-10,14-17].

View Article Online
DOI: 10.1039/D0DT01665A

The broth dilution method was used for the determination of the MIC values of **CIPTIN, HCIP·HCl**, **HCIP** and **DPTD**, upon incubation of Gram-negative (*P. aeruginosa* and *E. coli*) or Gram-positive (*S. aureus* and *S. epidermidis*) bacteria for 20 h (Table 1).

Table 1

The MIC values of **CIPTIN** lie in the range of nanomolar concentrations against *P. aeruginosa*, *E. coli, S. aureus* and *S. epidermidis*, (0.741±0.035, 0.301±0.062, 1.179±0.083 and 0.255±0.041 μM respectively) (Table 1, Figure S9). The corresponding MIC values of the drug in **HCIP·HCl** and **HCIP** are: 1.174±0.221 μM and 1.048±0.037 μM (*P. aeruginosa*), 0.938±0.347 μM and 0.443±0.041 μM (*E. coli*), 1.454±0.123 μM and 1.459±0.013 μM (*S. aureus*) and 1.079±0.121 μM and 0.699±0.025 μM (*S. epidermidis*), respectively (Figure S10-S11) [8]. The MIC values of **DPTD**, on the other hand, lie in the micromolar range of concentrations for the tested bacteria: >100 μM, 25.713±1.535 μM, 47.529±8.761 μM and 13.743±0.263 μM towards *P. aeruginosa*, *E. coli*, *S. aureus* and *S. epidermidis*, respectively (Figure S12). Thus, **CIPTIN** shows 1.2 to 4.2-folds stronger antimicrobial activity than those of **HCIP·HCl** or **HCIP** towards both Gram negative and positive bacteria. The strongest antimicrobial effect of **CIPTIN** is observed towards *S. epidermidis*, which is 4.2-fold higher than that of **HCIP·HCl** and 2.7 fold than that of **HCIP**. Moreover **CIPTIN** activity rises up to 135-folds than **DPTD** stronger activity against these bacteria. Therefore, **CIPTIN** exerts superior activity than both its ingredients (antibiotic and **DPTD**).

Microbes are classified to susceptible (MIC< 50 μM) or resistant (MIC> 100 μM) towards an antimicrobial agent by their MIC values [8,10]. Thus, all tested strains here are considered as susceptible to **CIPTIN**.

View Article Online
DOI: 10.1039/D0DT01665A

Table 1

Minimum bactericidal concentration (MBC): The MBC values for **CIPTIN** were also evaluated. MBC is defined as the lowest concentration of an antibacterial agent that kills the 99.9% of the initial bacterial inoculums [8,10,14-17].

The MBC values of **CIPTIN** for Gram negative *P. aeruginosa* and *E. coli* are 0.800±0.195 μM and 0.445±0.040 μM respectively, and against Gram positive bacteria *S. aureus*, and *S. epidermidis* are 1.600±0.110 μM and 0.667±0.045 μM, respectively (Table 1, Figure S13). The corresponding MBC values of **HCIP·HCl** and **HCIP** are 1.200-2.225 μM against both Gram negative and positive bacteria (Table 1, Figures S14-S15). In the case of **DPTD**, the MBC values are higher than 100 μM (Figure S16). Thus, **CIPTIN** exhibits higher bactericidal activity than those of free drugs which rises up to 3.6-fold in respect of **HCIP·HCl** or up to 2.8-fold for **HCIP**. **DPTD** has no bactericidal activity.

Since the MBC/MIC values of **CIPTIN** lie between 1.08-2.62, against the tested microbial strains, (Table 1) the **CIPTIN** is classified as bactericidal agent. This is because when the MBC/MIC value is ≤2, an agent is considered as bactericidal one, while when MBC/MIC value is ≥4, as bacteriostatic one [8,10,14-17]. The MBC/MIC values of **HCIP·HCl** and **HCIP** varied between 1.22-2.82 and they are bactericidal drugs.

Inhibition zone (IZ): The IZ was evaluated with agar disk-diffusion method [8,10,14-17]. The calculated diameter of IZ is used to determine the effectiveness of an antibiotic. Therefore, the bacterial strains might be classified as susceptible to an agent based on the IZ developed [8,10,14-17]. Thus, Shungu et.al [25] classified the microbes in three categories according to the size of IZ caused by antibiotics. (i) those strains where the antibiotic causes IZ ≥17 mm and they are consider as susceptible, (ii)

View Article Online
DOI: 10.1039/D0DT01665A

those where the antibiotic creates IZ between 13 to 16 mm (13 ≤ IZ ≤ 16 mm) are intermediate, (iii) those where the antibiotic causes IZ ≤ 12 mm, and they are considered as resistant strain [25].

The IZs caused by **CIPTIN** determined against *P. aeruginosa*, *E. coli*, *S. aureus* and *S. epidermidis* are 40.8±1.5, 34.0±0.8, 36.0±1.1 and 42.7±0.8 mm, respectively classifying these strains to susceptible ones towards **CIPTIN** (Figure 5). The ranges of IZs, which were caused by **HCIP·HCl** and **HCIP** lie between 32.0-35.5 mm (against Gram negative bacteria) and 24.0-39.2 mm (against Gram positive). These values are classifying the bacteria tested to susceptible ones against **HCIP·HCl** and **HCIP** (Table 1, Figure S17). The corresponding IZs developed by **DPTD** lie between 10.0-18.7 mm against the tested bacteria classifying them to the resistance or intermediate ones towards **DPTD**. Generally, **CIPTIN** causes greater inhibition zones than the commercial antibiotic or the **DPTD**, against both negative and positive bacterial strains.

Figure 5

Effect on biofilm formation by CIPTIN: The effect of **CIPTIN** on biofilm eradication was tested against biofilm-positive strains (*P. aeruginosa*, *S. aureus*) by the Biofilm Elimination Concentration (BEC) values with crystal violet assay [8-10,14-17]. The BEC is the required concentration to reduce the viability of biofilm bacteria by 99.9%, at least [8-10,14-17]. The BEC value of **CIPTIN** for *P. aeruginosa* is 656 μM and for *S. aureus* is 752 μM (Figure 6). We have recently determined the BEC value of **HCIP·HCl** against *P. aeruginosa* (670 μM) and *S. aureus* (952 μM) [8]. The corresponding BEC values of **HCIP** are: 2140 μM (*P. aeruginosa*) and 2463 μM (*S. aureus*) (Figure S19). **CIPTIN** eliminates the biofilm of *P. aeruginosa* and *S. aureus* more efficiently than the neutral drug **HCIP**, while its BEC value is comparable with the corresponding one of **HCIP·HCl**.

Figure 6

View Article Online
DOI: 10.1039/D0DT01665A

*Evaluation of the in vitro toxicity of **CIPTIN**:* Immortalized human keratinocytes (HaCaT) cells were used to test the *in vitro* cytotoxic effect of **CIPTIN**, **HCIP·HCl**, **HCIP** and **DPTD,** by sulforhodamine B (SRB) assay, upon their incubation with the agents by 48h. The IC_{50} value of **CIPTIN** is 2.33±0.2 μM. The corresponding IC_{50} values of H**CIP·HCl**, **HCIP** are >30 μM, while that of **DPTD** is 1.09±0.1 μM.

The therapeutic window of an agent is defined by the selectivity index (SI) [8,26]:

$$SI = IC_{50(\text{against HaCaT cells})}/MIC_{(\text{against tested bacteria})}$$

The higher SI is, the greater antimicrobial effect and lower the cellular toxicity is. The SI values of **CIPTIN** values are 3.1 (*P. aeruginosa*) 7.7 (*E. coli*), 2.0 (*S. aureus*) and 9.1 (*S. epidermidis*). These values constitute a wide therapeutic window for **CIPTIN**. The SI values of **DPTD** are: >0.01, 0.04, 0.02 and 0.08 against *P. aeruginosa*, *E. coli*, *S. aureus* and *S. epidermidis* respectively.

Evaluation of in vitro genotoxicity by micronucleus assay: The micronucleus assay is frequently used to evaluate the mutagenic, genotoxic or teratogenic effect of metallodrugs [27]. In the presence of a genotoxic factor, micronuclei (MN) appear as small membrane-bound DNA fragments in the cytoplasm of interphase cells and they are formed during the metaphase-anaphase transition of the mitotic cycle [28]. The micronucleus assay has been widely used in monitoring genetic damage in order to avoid the screening of drugs on animals.

In order to evaluate the genotoxicity of **CIPTIN**,·**HCIP·HCl**, **HCIP** and **DPTD**, HaCaT cells were treated by the agents at their IC_{50} values (Figure 7). The corresponding frequency of micronucleus after treatment of HaCaT cells by **CIPTIN** is 2.60±0.15 %, while the frequency without treatment of the cells is 2.17±0.05 %. Therefore **CIPTIN** exhibits negligible genotoxicity. The micronucleus frequencies of HaCaT cells after treatment by the **HCIP·HCl** (2.44±0.2)% or **HCIP** (2.48±0.1)% which is close to that of **CIPTIN**. The MN formed upon treatment of HaCaT cells by **DPTD** is (3.05±0.2) %, which is significantly higher than that of **CIPTIN**.

View Article Online
DOI: 10.1039/D0DT01665A

Figure 7

Conclusions

The design and the development of antimicrobial agents are of great importance. The new metalloantibiotic **CIPTIN**, has been synthesized and characterized within this work. The crystal structure reveals that the geometry around the metal center is octahedral (Figure 1B). The stereoselective synthesis results to the Δ-*cis*-[$Ph_2Sn(CIP)_2$] isomer only (Figure 1B). 2D layers supramolecular assemblies are established based on strong hydrogen bonding interactions (Figure 3). Four molecules form squares planes with their tins atoms to occupy its acnes of each square. These constitute the building blocks of the layers (Figure 3). The area is covered by each square is 195.133 $Å^2$.

CIPTIN has been evaluated towards the Gram negative microbes *P. aeruginosa*, *E. coli* and Gram positive ones *S. aureus*, *S. epidermidis*. **CIPTIN** is classified as a bactericidal agent against *P. aeruginosa*, *E. coli*, *S. aureus* and *S. epidermidis* (Table 1), while these microbes, are ranked among the susceptible ones to it (IZ values) (Table 1).

The antibacterial activity of **CIPTIN** (Δ-*cis*-[$Ph_2Sn(CIP)_2$]) is compared with those of **CIPAG** with formula ({[$Ag(HCIP)_2$]NO_3·}) [8], [$Me_3Sn(CIP)$], [$Cy_3Sn(CIP)$] [13] and **PenAg** with formula [$Ag(Pen)(CH_3OH)]_2$, (HPen= penicillin) [9] and their ingredients **HCIP·HCl**, **HCIP**, **PenNa**, **DPTD** and $AgNO_3$ (Table 1, Figure 8).

CIPTIN exhibits stronger activity than ciprofloxacin against both Gram positive and negative bacteria tested as well as the [$Me_3Sn(CIP)$], [$Cy_3Sn(CIP)$] [13] suggesting that the presence of the tin(IV) ion enhances ciprofloxacin's effectiveness even more (Table 1, Figure 8). While **DPTC's** activity is significant lower than that of **CIPTIN,** this should be attributed to the synergistic effect of both the organotin moiety and ciprofloxacin. **CIPTIN** exerts superior activity than penicillin against Gram negative, as expected since penicillin is inactive against Gram negative

View Article Online
DOI: 10.1039/D0DT01665A

bacteria microbes (Figure 8). Against Gram positive microbes, **CIPTIN** exhibits stronger activity against *S. epidermidis* while penicillin shows higher one on *S. aureus* (Figure 8). Given that ciprofloxacin exhibits stronger activity than penicillin against *S. epidermidis*, while penicillin against *S. aureus*, **CIPTIN** follows the relative efficiency of ciprofloxacin towards penicillin. Among the compounds of ciprofloxacin, **CIPTIN** exhibits higher activity from **CIPAG** against *S. epidermidis*, which however is more effective against *S. aureus* and *P. aeruginosa* (Figure 8). Therefore, the antibiotic activity is differentiated by the type of the metal ion which is coordinating on the drug. Moreover, among organotins, the [Me_3Sn(CIP)] and the [Cy_3Sn(CIP)] [13] show stronger activity than **CIPTIN** against *P. aeruginosa* and *S. aureus* (Table 1). However this should be assigned to the higher toxicity of tri- than di-organotin moieties. Although **PenAg** shows better activity against *S. aureus,* **CIPTIN**, however is more drastic against *S. epidermidis* and *P. aeruginosa* where ciprofloxacin itself shows better activity than free penicillin (Figure 8). Therefore the activity of the metallodrug is following the corresponding efficiency of the antibiotic, regardless the type of the metal ion Sn(IV) or Ag(I). Moreover **CIPTIN** shows superior activity than silver(I) nitrate against all microbes tested (Figure 8) confirming the conclusion which is already withdrawn for the synergy of the metal ion with the drug on the activity of the metallodrug. **CIPTIN** eliminates the biofilm in a similar manner with the drug (Table 1). The *in vitro* toxicity of the **CIPTIN** against HaCaT cells shows a selectivity index (SI) higher than 1 suggesting wide therapeutic window, while its *in vitro* genotoxicity is even lower than that of **HCIP·HCl** or **HCIP.**

In conclusion, the coordination of a drug on a metal ion strongly enhances its activity. The antimicrobial information which has been stored in a drug, affects the activity of the metallodrug and it is affected by the coordination demands stored in the metal ion, creating a combination of a new entity with enhance and novel biological properties.

Figure 8

Experimental

View Article Online
DOI: 10.1039/D0DT01665A

Materials and instruments: All solvents used were of reagent grade. Tryptone tryptophan medium, beef extract powder, peptone bacteriological, soy peptone were purchased from Biolife. Agar and yeast extract were purchased from Fluka Analytical. Sodium chloride, D(+)-Glucose, di Potassium hydrogen phosphate trihydrate were purchased from Merck. Dulbecco's modified Eagle's medium, (DMEM), fetal bovine serum, glutamine and trypsin were purchased from Gibco, Glasgow, UK. Phosphate buffer saline (PBS) was purchased from Sigma-Aldrich. Melting points were measured in open tubes with a Stuart Scientific apparatus and are uncorrected. IR spectra in the region of 4000-370 cm^{-1} were obtained on Cary 670 FTIR spectrometer, Agilent Technologies. A UV-1600 PC series spectrophotometer of VWR was used to obtain electronic absorption spectra. The ^{1}H-NMR spectra were recorded on a Bruker AC 250, 400 MHFT-NMR instrument in DMSO-d_6. ESI-MS spectra were measured with an Agilent 1100/LC−MS system. ^{119}Sn Mössbauer spectra were collected at various sample temperatures (85 K), with a constant-acceleration spectrometer equipped with a $CaSnO_3$ source kept at room temperature. The calibration of the spectrometer was carried out with a ^{57}Co source and an Fe absorber at room temperature. The line widths were very close to the natural width (0.28 mm/s). The content of the tin samples was calculated to be approximately 4 mg Sn in the 2-cm^2 area of the sample holder. XRF measurements were carried out using an Am-241 radio isotopic source (exciting radiation 59.5 keV). Thermal Gravimetric–Differential Thermal Analysis (TG–DTA) of **CIPTIN** was carried out on a Seiko SII TG/DTA 7200 apparatus under N_2 flow (40 cm^3 min^{-1}) with a heating rate of 10 K min^{-1}.

Synthesis and crystallization of CIPTIN: A clear solution of 0.5 mmol ciprofloxacin hydrochloride (**HCIP·HCl**) (0.184 gr) in dd water (8 mL) was treated with 0.75 mmol KOH (750 µL 1 N). A solution of 0.25 mmol diphenyltin dichloride (**DPTD**) (0.086 gr) in methanol (3 mL) was added to the previous one under continues stirring for 30 min and the resulting white precipitation was

View Article Online
DOI: 10.1039/D0DT01665A

immediately filtered off. Crystals of **CIPTIN** suitable for X-ray analysis were grown from slow evaporation of the solution after one day.

CIPTIN: Yellowish crystal, melting point: > 300 °C; elemental analysis found: C: 59.55; H: 4.92, N: 9.23%; calculated for $C_{46}H_{44}N_6O_6F_2Sn$: C: 59.19; H: 4.75; N:9.00 %. IR (cm^{-1}), (KBr): 3906w, 2965w, 2698w, 2487w, 2111w, 1918w, 1604w, 1474w, 1265s, 1142s, 1025s, 944vs, 809s, 739vs, 628s, 446s; ^{1}H-NMR (ppm) in DMSO-d_6: 8.87 (s, H[Npiperazine ring]), 8.67 (s, H[^{2}C]), 7.95-7.92 (d, H[^{5}C]), 7.79-7.81 (d, H[^{8}C]), 7.72-7.58 (m, Ph-), 7.31-7.16 (m, Ph-), 3.85 (s, H[^{a}C]), 3.47 (d, H[^{c}C]), 1.33 (m, cyclopropyl CH_2), 1.19 (m, cyclopropyl CH_2); UV-vis (DMSO): λ= 284 nm (logε= 4.68), λ= 320 nm (logε= 4.21), 331 nm, (logε= 4.20).

X-ray Structure Determination: Intensity data for the crystals of **CIPTIN** and **HCIP** were collected on an Oxford Diffraction CCD instrument, using graphite monochromated Mo radiation (λ=0.71073 Å). Cell parameters were determined by least-squares refinement of the diffraction data from 25 reflections. All data were corrected for Lorentz-polarization effects and absorption [29]. The structures were solved with direct methods with SHELXS97 [30] and refined by full-matrix least-squares procedures on F^2 with SHELXL97 [31]. All non-hydrogen atoms were refined anisotropically, hydrogen atoms were located at calculated positions and refined via the "riding model" with isotropic thermal parameters fixed at 1.2 (1.3 for CH_3 groups) times the Ueq value of the appropriate carrier atom.

CIPTIN: $C_{46}H_{44}N_6O_6F_2Sn$, MW= 933.612, monoclinic, space group I2/a, a= 14.7410(6), b= 20.2602(5), c= 18.8558(7) Å, α= 90, β= 111.400(4), γ= 90°, V= 5243.1(3) Å^3, Z= 4, T= 100 K, ρ (calc)= 1.183 g cm^{-3}, μ= 4.320 mm^{-1}, F(000)= 1912. 10180 reflections measured, 4682 unique (Rint = 0.052). The final R1= 0.0523 (for 3818 reflections with I > 2s(I)) and wR(F2)= 0.1428 (all data) S= 0.99.

HCIP: $C_{17}H_{18}FN_3O_3$, MW= 331.34, triclinic, space group P-1, a= 7.8945(7), b= 8.5010(7), c= 10.7522(9) Å, α= 87.440(7), β= 84.496(7), γ= 88.912(7)°, V= 717.47(11) Å^3, Z= 2, T= 100 K, ρ

View Article Online
DOI: 10.1039/D0DT01665A

(calc)= 1.534 g cm^{-3}, μ= 0.967 mm^{-1}, F(000)= 348. 4189 reflections measured, 2531unique (Rint = 0.041). The final R1= 0.0511 (for 1996 reflections with I > 2s(I)) and wR(F2)= 0.1440 (all data) S= 1.07.

Crystallographic data (excluding structure factors) for the structure reported in this paper has been deposited with the Cambridge Crystallographic Data Centre as supplementary publication nos. CCDC-1993746 (**CIPTIN**), CCDC-2002394 (**HCIP**). Copies of the data can be obtained free of charge on application to CCDC, 12 Union Road, Cambridge CB2 1EZ, UK (fax: (+44) 1223-336-033; e-mail: deposit@ccdc.cam.ac.uk).

Biological tests:

Bacterial Strains: The strains used were: *Pseudomonas aeruginosa* (*P. aeruginosa*), *Escherichia coli Dh5a (E. coli)*, *Staphylococcus aureus* (*S. aureus*) subsp. aureus (ATCC® 25923™) and *Staphylococcus epidermidis* (ATCC® 14990™).

Solvents used: The biological experiments for antibacterial studies were carried in DMSO/Broth solutions of **CIPTIN**, **HCIP** and **DPTD** and in H_2O/Broth solutions for **HCIP·HCl**. The biological experiments for the cell viability and for the micronucleus assay were carried in DMSO/DMEM solutions 0.0005-0.03% v/v DMSO in DMEM for the tested compounds. Stock solutions of **CIPTIN**, H**CIP·HCl**, **HCIP** and **DPTD** (0.01 M) in DMSO were freshly prepared and diluted in broth or cell culture medium to the desired concentration.

Minimum inhibitory concentration (MIC) testing: This study was performed according standard procedure, as described previously [8-10,14-17]. Briefly, the bacterial strains were streaked onto in trypticase soy agar plates, which were incubated for 18-24 h at 37 °C. Then, three to five isolated colonies were selected of the same morphological appearance from the fresh agar plate using a sterile loop and transferred into a tube containing 2 mL of sterile saline solution. The optical density at 620 nm is 0.1, which corresponds in to 10^8 cfu/mL. The final inoculum size for broth dilution is

View Article Online
DOI: 10.1039/D0DT01665A

5×10^5 cfu/mL. The total volume of the culture solution treated by **CIPTIN**, **HCIP·HCl**, **HCIP** or **DPTD**, and the total volumes of the positive and negative controls, were 2 mL. The range of concentrations of **CIPTIN** was 100-1600 nM, of **HCIP·HCl** was 100-800 nM, of **CIPH** was 200-1600 nM and of **DPTD** was 5000-100000 nM. The growth was assessed after incubation for 20 h. The MIC value was determined as the concentration of the compound which inhibits the visible growth of the bacterium being investigated, while it confirmed by measuring the solution optical density at 620 nm *vs* concentrations [8-10,14-17].

Minimum bactericidal concentration testing: In order to determine MBC values of **CIPTIN**, the bacteria were initially cultivated in the presence of **CIPTIN**, **HCIP·HCl**, **HCIP** or **DPTD** in broth for 20 h. Afterwards, MBC value was determined in duplicate, by subculturing 4 μL of the broth with bacteria and **CIPTIN**, **HCIP·HCl**, **HCIP** or **DPTD** in an agar plate. Bactericidal activity occurs when no colony formation is observed. The lowest concentration at which the tested compounds could give complete inhibition of microbes' growth was defined as MBC value [8-10,14-17].

Determination of the inhibition zone (IZ) through the agar disk-diffusion method: As described previously [8-10,14-17], agar plates were inoculated with a standardized inoculum (10^8 cfu/mL) of the tested microorganism. Filter paper disks (9 mm in diameter), which had been previously soaked by **CIPTIN**, **HCIP·HCl**, **HCIP or DPTD** (10^{-3} M), were placed on the agar surface. The Petri dishes were incubated for 20 h, and then the diameters of the inhibition zones were measured.

Effects on biofilm formation: Bacterial strains of *P. aeruginosa* or *S. aureus* with a density of 6.7×10^6 cfu/mL were inoculated into LB medium (total volume= 1500 μL) and cultured for 24 h at 37 °C. Afterwards, the content of each tube was carefully removed and the tubes are washed with 1 mL dH_2O. Negative control contained broth only. Then, the bacteria were incubated with **CIPTIN** at concentrations between 25 to 500 μM (total volume= 2000 μL) for 20 hrs, at 37 °C. The content of each tube was aspirated, each tube was washed three times with 1 mL methanol and 2 mL ddH_2O and left to dry. Then, the tubes were stained for 15 min with crystal violet solution (0.1% w/v).

View Article Online
DOI: 10.1039/D0DT01665A

Excess stain was rinsed off with 1 mL methanol and 2 mL ddH_2O. The tubes are left to dry for 24 hand the bounded crystal violet was released by adding 30% glacial acetic acid (2 mL) and after 3 mL ddH_2O. The optical density of the solution yielded is measured at 550 nm, to give the biofilm biomass [8-10,14-17].

In vitro toxicity evaluation

Sulforhodamine B Assay: These studies were performed in accordance with the previous reported method [10,15]. Briefly, HaCaT cells were seeded in 96-well plate in a density of 8000 cells and after 24 h of cell incubation, the compounds were added in the range of concentration 0.25-3 μM (for **CIPTIN** and **DPTD**) and 0.5-30 μM (for **HCIP·HCl** and **HCIP**). After of 48 h incubation of HaCaT cells with the compounds, the culture medium was aspirated and the cells were fixed with 50 μL of 10% cold trichloroacetic acid (TCA). The plate was left for 30 min at 4 °C, washed five times with deionized water, and left to dry at room temperature for at least 24 h. Subsequently, 70 μL of 0.4% (w/v) sulforhodamine B (Sigma) in 1% acetic acid solution was added to each well and left at room temperature for 20 min. SRB was removed, and the plate was washed five times with 1% acetic acid before air drying. Bound SRB was solubilised with 200 μL of 10 mM un-buffered Tris-base solution. Absorbance was read in a 96-well plate reader at 540 nm.

Evaluation of genotoxicity by micronucleus assay: The micronucleus assay was carried out as previously described [27]. Briefly HaCaT cells were seeded (at a density of 240000 cells/well) in glass cover slips which were afterwards placed in six-well plates, with 3 mL of cell culture medium and incubate for 24 h. HaCaT cells exposed with compounds in IC_{50} values for a period of 48 h. The number of micronucleated cells per 1000 cells was determined.

Acknowledgements

[i] This research has been co-financed by the European Union and Greek national funds through the Operational Program Competitiveness, Entrepreneurship and Innovation, under the call

RESEARCH – CREATE – INNOVATE (project code:T1EDK- 02990). [ii] This research is also co-financed by Greece and the European Union (European Social Fund- ESF) through the Operational Programme «Human Resources Development, Education and Lifelong Learning» in the context of the project “Strengthening Human Resources Research Potential via Doctorate Research” (MIS-5000432), implemented by the State Scholarships Foundation (IKY). [iii] Professor T. Vaimakis is acknowledged for the useful discussions and the recording of TG-DTA/DSC diagrams. [iv] The COST Action CA15114 "Anti-Microbial Coating Innovations to prevent infectious diseases (AMICI)" is acknowledged for the stimulating discussions.

References

View Article Online
DOI: 10.1039/D0DT01665A

[1] N.R. Cozzarelli, DNA gyrase and the supercoiling of DNA, Science, 1980, 207, 953–960.

[2] M. Brunner, O. Langer, G. Dobrozemsky, U. Muller, M. Zeitlinger, M. Mitterhauser, W. Wadsak, R. Dudczak, K. Kletter, M. Müller, [18F] Ciprofloxacin, a new positron emission tomography tracer for noninvasive assessment of the tissue distribution and pharmacokinetics of ciprofloxacin in humans. Antimicrob Agents Chemother, 2004, 48, 3850–3857

[3] F. Silva, O. Lourenço, J.A. Queiroz, F.C. Domingues, Bacteriostatic versus bactericidal activity of ciprofloxacin in Escherichia coli assessed by flow cytometry using a novel far-red dye, J Antibiot, 2011, 64, 321–325

[4] M. Mulder, J.C. Kiefte-de Jong, W.H. Goessens, H. de Visser, A. Hofman, B.H. Stricker, A. Verbon, Risk factors for resistance to ciprofloxacin in community-acquired urinary tract infections due to Escherichia coli in an elderly population. J Antimicrob Chemother, 2017, 72, 281-289

[5] J. Overgaard, I. Turel, D.E. Hibbs, Experimental electron density study of a complex between copper(ii) and the antibacterial quinolone family member ciprofloxacin, Dalton Trans., 2007, 2171–2178

[6] P. Drevensek, T. Zupancic, B. Pihlar, R. Jerala, U. Kolitsch, A. Plaper, I. Turel, Mixed-valence Cu(II)/Cu(I) complex of quinolone ciprofloxacin isolated by a hydrothermal reaction in the presence of L-histidine: comparison of biological activities of various copper-ciprofloxacin compounds., J. Inorg. Biochem., 2005, 99, 432–442

[7] P. Drevensek, N. Poklar Ulrih, A. Majerle, I. Turel, Synthesis, characterization and DNA binding of magnesium-ciprofloxacin (cfH) complex [Mg(cf)2] * 2.5H2O., J. Inorg. Biochem., 2006, 100, 1705–1713

[8] I. Milionis, C.N. Banti, I. Sainis, C.P. Raptopoulou, V. Psycharis, N. Kourkoumelis, S.K. Hadjikakou, Silver ciprofloxacin (CIPAG): a successful combination of chemically modified antibiotic in inorganic–organic hybrid, J Biol Inorg Chem, 2018, 23, 705–723

View Article Online
DOI: 10.1039/D0DT01665A

[9] I. Ketikidis, C.N. Banti, N. Kourkoumelis, C.G. Tsiafoulis, C. Papachristodoulou, A.G. Kalampounias, S.K. Hadjikakou, Conjugation of Penicillin-G with Silver(I) Ions Expands Its Antimicrobial Activity against Gram Negative Bacteria, Antibiotics, 2020, 9, 25

[10] M.P. Chrysouli, C.N. Banti, I. Milionis, D. Koumasi, C.P. Raptopoulou, V. Psycharis, I. Sainis, S.K. Hadjikakou, A water-soluble silver(I) formulation as an effective disinfectant of contact lenses cases, Mater. Sci. Eng. C, 2018, 93, 902–910

[11] P. J. Smith, Chemistry of Tin, 2nd edn, (ed) Blackie Academic & Professional, London, 1997 ISBN 0-7514-0385-7

[12] A.G. Davies, Organotin Chemistry, 2004, 2nd Edition, Wiley-VCH Verlag GmbH & Co. KGaA

[13] R. Joshi, S.K. Yadav, H. Mishra, N. Pandey, R. Tilak, S. Pokharia, Interaction of triorganotin(IV) moiety with quinolone antibacterial drug ciprofloxacin: Synthesis, spectroscopic investigation, electronic structure calculation, and biological evaluation, Heteroatom Chem., 2018, 29, 21433

[14] I. Sainis, C.N. Banti, A.M. Owczarzak, L. Kyros, N. Kourkoumelis, M. Kubicki S.K. Hadjikakou, New antibacterial, non-genotoxic materials, derived from the functionalization of the anti-thyroid drug methimazole with silver ions, J. Inorg. Biochem., 2016, 160, 114–124.

[15] M.K. Stathopoulou, C.N. Banti, N. Kourkoumelis, A.G. Hatzidimitriou, A.G. Kalampounias, S.K. Hadjikakou, Silver complex of salicylic acid and its hydrogel- cream in wound healing chemotherapy, J. Inorg. Biochem., 2018, 181, 41–55

[16] A. Papadimitriou, I. Ketikidis, M.-E.K. Stathopoulou, C.N. Banti, C. Papachristodoulou, L. Zoumpoulakis, S. Agathopoulos, G.V. Vagenas, S.K. Hadjikakou, Innovative material containing the natural product curcumin, with enhanced antimicrobial properties for active packaging, Mater. Sci. Eng. C, 2018, 84, 118–122

[17] V.A. Karetsi, C.N. Banti, N. Kourkoumelis, C. Papachristodoulou, C.D. Stalikas, C.P. Raptopoulou, V. Psycharis, P. Zoumpoulakis, T. Mavromoustakos, I. Sainis, S.K.

Hadjikakou, An Efficient Disinfectant, Composite Material {SLS@[Zn3(CitH)2]} as Ingredient for Development of Sterilized and Non Infectious Contact Lens, Antibiotics, 2019, 8, 213

View Article Online
DOI: 10.1039/D0DT01665A

[18] F.P.A. Fabbiani, B. Dittrich, A.J. Florence, T. Gelbrich, M.B. Hursthouse, W.F. Kuhs, N. Shankland, H. Sowa, Crystal structures with a challenge: high-pressure crystallisation of ciprofloxacin sodium salts and their recovery to ambient pressure, CrystEngComm, 2009, 11, 1396–1406

[19] C.N. Banti, E.I. Gkaniatsou, N. Kourkoumelis, M.J. Manos, A.J. Tasiopoulos, T. Bakas, S.K. Hadjikakou, Assessment of organotins against the linoleic acid, glutathione and CT-DNA, Inorg Chim Acta, 2014, 2014, 423, 98-106

[20] S.K. Hadjikakou, M.A. Abdellah, N. Hadjiliadis, M. Kubicki, T. Bakas, N. Kourkoumelis, Y.V. Simos, S. Karkabounas, M.M. Barsan, I.S. Butler, Synthesis, characterization, and biological studies of organotin(IV) derivatives with o- or p-hydroxybenzoic acids, Bioinorg Chem Appl., 2009, art. no. 542979

[21] M.N. Xanthopoulou, S.K. Hadjikakou, N. Hadjiliadis, M. Kubicki, S. Skoulika, T. Bakas, M. Baril, I.S. Butler, Synthesis, structural characterization, and biological studies of six- and five-coordinate organotin(IV) complexes with the thioamides 2- mercaptobenzothiazole, 5-chloro-2-mercaptobenzothiazole, and 2-mercaptobenzoxazole, Inorg Chem, 2007, 46, 1187

[22] M.N. Xanthopoulou, S.K. Hadjikakou, N. Hadjiliadis, M. Schürmann, K. Jurkschat, A. Michaelides, S. Skoulika, T. Bakas, J. Binolis, S. Karkabounas, K. Charalabopoulos, Synthesis, structural characterization and in vitro cytotoxicity of organotin(IV) derivatives of heterocyclic thioamides, 2-mercaptobenzothiazole, 5-chloro-2-mercaptobenzothiazole, 3-methyl-2-mercaptobenzothiazole and 2-mercaptonicotinic acid, J. Inorg. Biochem., 2003, 96, 425-434

[23] P. Pachori, R. Gothalwal, P. Gandhi, Emergence of antibiotic resistance Pseudomonas aeruginosa in intensive care unit; a critical review, Genes & Diseases, 2019, 6, 109-119

View Article Online
DOI: 10.1039/D0DT01665A

[24] M. Otto, Staphylococcus epidermidis – the "accidental" pathogen, Nat Rev Microbiol. 2009, 7, 555–567

[25] D.L. Shungu, E. Weinberg, H.H. Gadebusch, Tentative interpretive standards for disk diffusion susceptibility testing with norfloxacin (MK-0366, AM-715), Antimicrob. Agents Chemother., 1983, 23, 256 –260

[26] M.P. Pereira, S.O. Kelley, Maximizing the therapeutic window of an antimicrobial drug by imparting mitochondrial sequestration in human cells. J Am Chem Soc, 2011, 133, 3260–3263

[27] C.N. Banti, S.K. Hadjikakou, Evaluation of Genotoxicity by Micronucleus Assay in vitro and by Allium cepa Test in vivo, Bio-protocol, 2019, 9, e3311

[28] M. Fenech, The micronucleus assay determination of chromosomal level DNA damage, Methods Mol. Biol., 2008, 410, 185–216

[29] CrysAlis RED, version 1.171.31.5; Oxford Diffraction Ltd., 2006 (release 28-08- 2006 CrysAlis171.NET), Oxford Diffraction, Crysalis CCD and Crysalis RED, Version p171.29.2, Oxford Diffraction Ltd., Abingdon, Oxford, England, 2006

[30] G.M. Sheldrick, Phase annealing in SHELX-90: direct methods for larger structures, Acta Crystallogr. A, 1990, 46, 467

[31] G.M. Sheldrick, SHELXL-97, Program for the Refinement of Crystal Structures, University of Göttingen, Göttingen, Germany, 1997

Figure Captions

View Article Online
DOI: 10.1039/D0DT01665A

Figure 1. **(A)** Molecular diagram together with the numbering scheme of **CIPTIN**. Selected bond lengths (Å) and angles [°]: Sn1-O1= 2.135(3), Sn1-O3= 2.158(3), Sn1-C18= 2.120(5), Sn1-O1_a= 2.135(3), Sn1-O3_a= 2.158(3), Sn1-C18_a= 2.120(5), O3-C2= 1.284(5), O1-C6= 1.298(5), O2-C6= 1.216(5), O1-Sn1-O3= 79.93(11), O1-Sn1-O1_a= 155.64(11), O1-Sn1-O3_a= 81.60(11), O1_a-Sn1-O3= 81.60(11), O3-Sn1-O3_a= 80.96(11), O1_a-Sn1-O3_a= 79.93(11). **(B)** Δ-*cis*-[$Ph_2Sn(CIP)_2$] stereoisomer

Figure 2. **(A)** Molecular diagram together with the numbering scheme of **HCIP**. Selected bond lengths (Å) and angles [°]:O1-C14= 1.247(3), O2-C14= 1.266(3), C1-C2= 1.453(3), O3-C2= 1.241(3), N3-C11= 1.481(3), N3-C12= 1.485(3), O1-C14-O2= 125.3(2), O3-C2-C1= 125.0(2), C11-N3-C12= 109.0(2) (B) 1D ribbon assembly established by hydrogen bonds

Figure 3 Strong hydrogen bonding interactions O2[H2]···N3 lead to 2D layer architecture.

Figure 4 ^{119}Sn Mössbauer spectrum of **CIPTIN** at 77 K.

Figure 5. Inhibition zones of **CIPTIN** against *P. aeruginosa* (A), *E. coli* (B), *S. aureus* (C) and *S. epidermidis* (D)

Figure 6. Crystal violet staining revealing biofilm *P. aeruginosa* (A) and *S. aureus* (B) with increasing concentrations of **CIPTIN**. Biofilm inhibition (%) of *P. aeruginosa* and *S. aureus* versus pC=-log(C) (M) of **CIPTIN** (C).

Figure 7. Representative snapshots of micronucleus formed in untreated HaCaT cells (A) and upon their treatment with **CIPTIN** (B), **HCIP·HCl** (C), **HCIP** (D) or **DPTD** (E) at 2.33 μM for 48 h.

Figure 8. Istogramm of pMIC (-log(MIC)) values of **CIPTIN** (Δ-*cis*-[$Ph_2Sn(CIP)_2$]), ({[$Ag(HCIP)_2$]NO_3·}) [8], **PenAg** [Ag(Pen)(CH_3OH)]$_2$, (HPen= penicillin) [9], **HCIP·HCl**, **HCIP**, **PenNa**, **DPTD** and $AgNO_3$, against *S. aureus, S. epidermidis, P. aeruginosa* and *E. coli*.

Table 1. MIC, MBC values, Inhibition Zones, of **CIPTIN**, **CIPAG, PenAg, HCIP·HCl**, **HCIP, DPTD** and **$AgNO_3$** against *P. aeruginosa*, *E. coli*, *S. aureus* and *S. epidermidis*

View Article Online
DOI: 10.1039/D0DT01665A

Compound	*P. aeruginosa*	*E. coli*	*S. aureus*	*S. epidermidis*	Ref.
MIC (μM)					
$Ph_2Sn(CIP)_2$ CIPTIN	0.741±0.035	0.301±0.062	1.179±0.083	0.255±0.041	*
Me_3SnCIP	0.253	1.012	0.125	-	[13]
Cy_3SnCIP	0.089	1.432	0.179	-	[13]
$Ag(CIP)_2NO_3$ CIPAG	0.612±0.142	-	0.537±0.067	0.458±0.083	[8]
$[Ag(Pen)](DMSO)]_2$	23.0±2.290	-	0.080±0.020	2.410±0.880	[9]
HCIP·HCl	1.174±0.221	0.938±0.347	1.454±0.123	1.079±0.121	[8]
HCIP	1.048±0.037	0.443±0.041	1.459±0.013	0.699±0.025	*
PenNa	>2000	-	0.140±0.020	3.760±1.140	[9]
Ph_2SnCl_2 DPTD	> 100	25.713±1.535	47.529±8.761	13.743±0.263	*
$AgNO_3$	60.0	-	79.500	39.400	[8]
MBC (μM)					
$Ph_2Sn(CIP)_2$ CIPTIN	0.800±0.195	0.445±0.040	1.600±0.110	0.667±0.045	*
Me_3SnCIP	0.506	1.012	0.506	-	[13]
Cy_3SnCIP	0.716	2.863	0.358	-	[13]
$Ag(CIP)_2NO_3$ CIPAG	0.700	-	1.000	0.800	[8]
$[Ag(Pen)](DMSO)]_2$	46.6	-	-	-	[9]
HCIP·HCl	1.6	1.624±0.127	2.000	1.600	[8]
HCIP	1.280±0.096	1.250±0.098	2.225±0.050	1.200±0.160	*
PenNa	2000	-	-	-	[9]
Ph_2SnCl_2 DPTD	> 100	> 100	> 100	> 100	*
$AgNO_3$	91.5		95.0	140.0	[8]
MBC/MIC					
$Ph_2Sn(CIP)_2$ CIPTIN	1.08	1.48	1.36	2.62	*
Me_3SnCIP	2.0	1.0	4.05	-	[13]
Cy_3SnCIP	8.04	2.0	2.0	-	[13]
$Ag(CIP)_2NO_3$ CIPAG	1.14	-	1.86	1.75	[8]
HCIP·HCl	1.36	1.73	1.38	1.48	[8]
HCIP	1.22	2.82	1.53	1.72	*
$AgNO_3$	1.53		1.19	3.55	[8]
IZ (mm)					
$Ph_2Sn(CIP)_2$ CIPTIN	40.8 ± 1.5	34.0 ± 0.8	36.0 ±1.1	42.7 ± 0.8	*
$Ag(CIP)_2NO_3$ CIPAG	32	-	28	34	[8]
$[Ag(Pen)](DMSO)]_2$	17	-	57	34	[9]
HCIP·HCl	32.0	32.0 ± 0.8	24.0	36.0	[8]
HCIP	35.5 ± 0.6	33.0 ± 0.8	30.5 ± 0.6	39.2 ± 0.9	*
PenNa	10	-	60	34	[9]
Ph_2SnCl_2 DPTD	10.0± 0.0	18.7 ± 0.9	13.1 ± 0.6	15.8± 0.4	*
$AgNO_3$	13		12	14	[8]

* This study, **PenNa**= sodium salt of penicillin

View Article Online
DOI: 10.1039/D0DT01665A

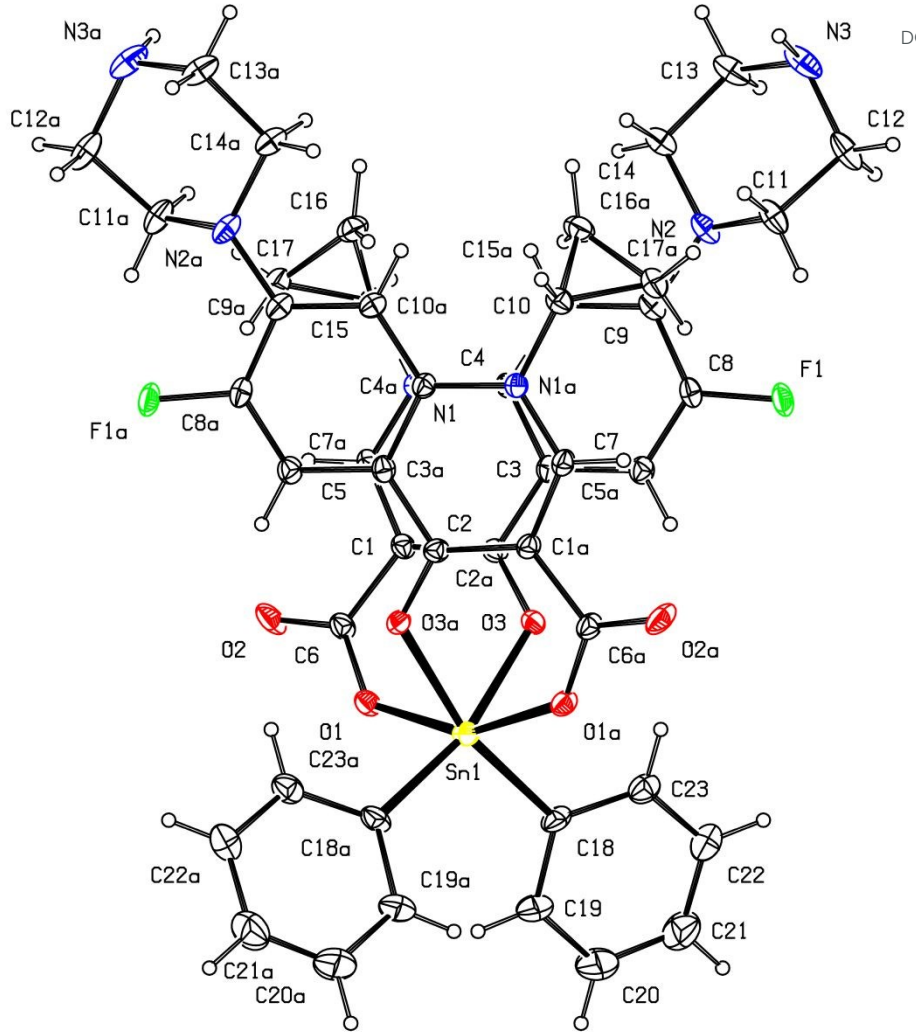

(A)

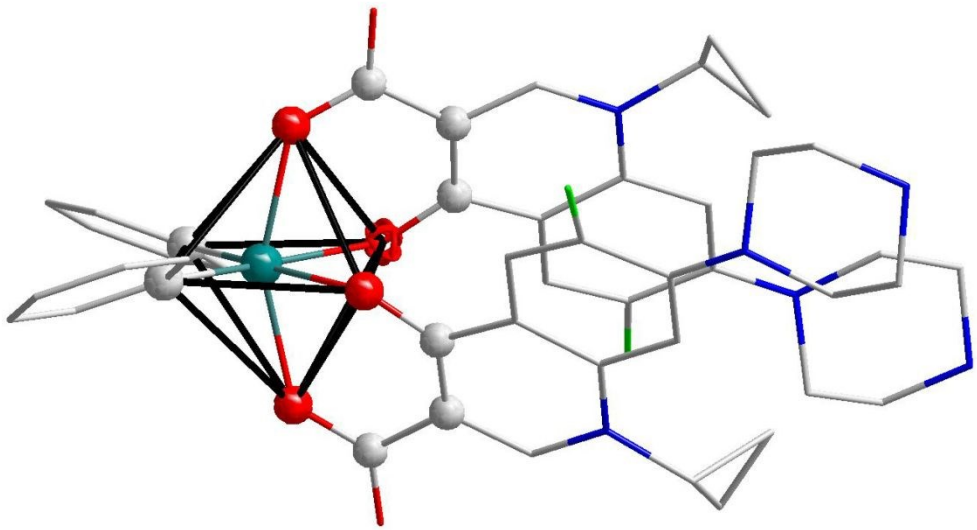

(B)

Figure 1

View Article Online
DOI: 10.1039/D0DT01665A

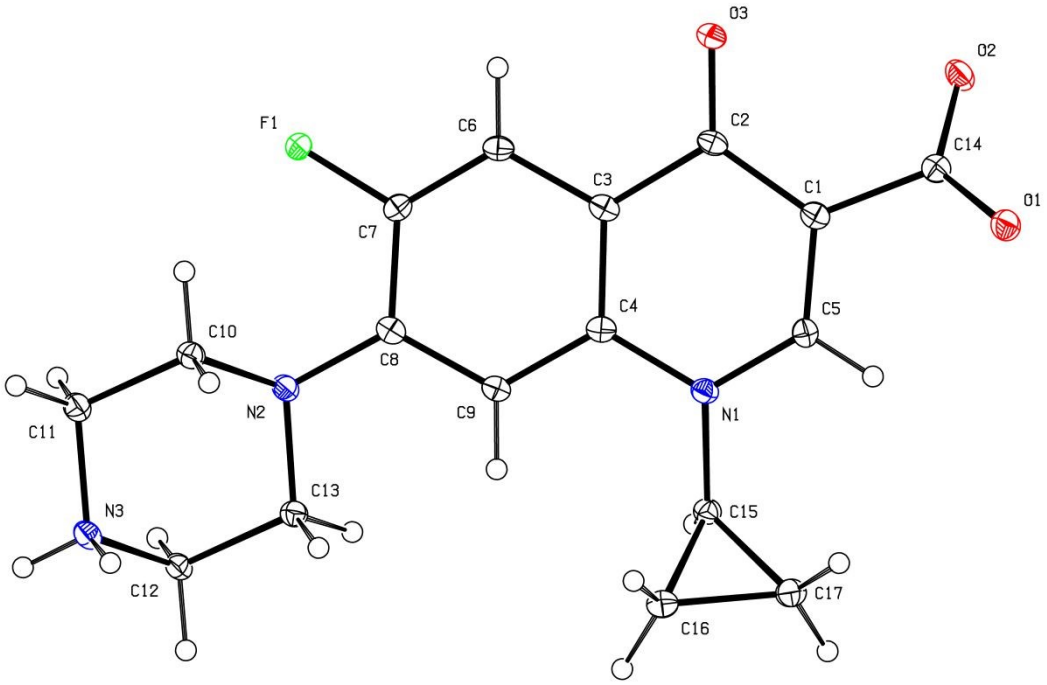

(A)

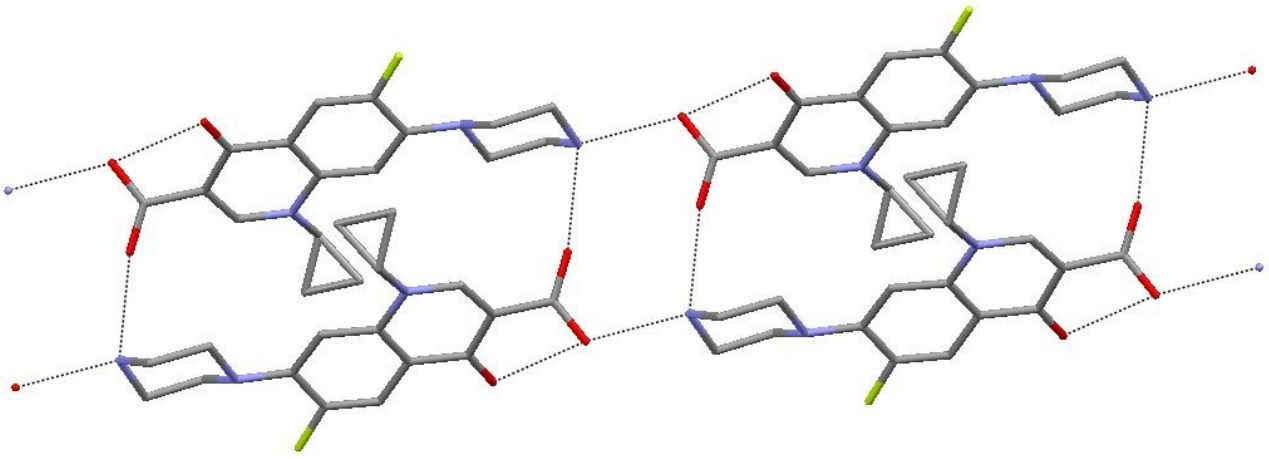

(B)

Figure 2

View Article Online
DOI: 10.1039/D0DT01665A

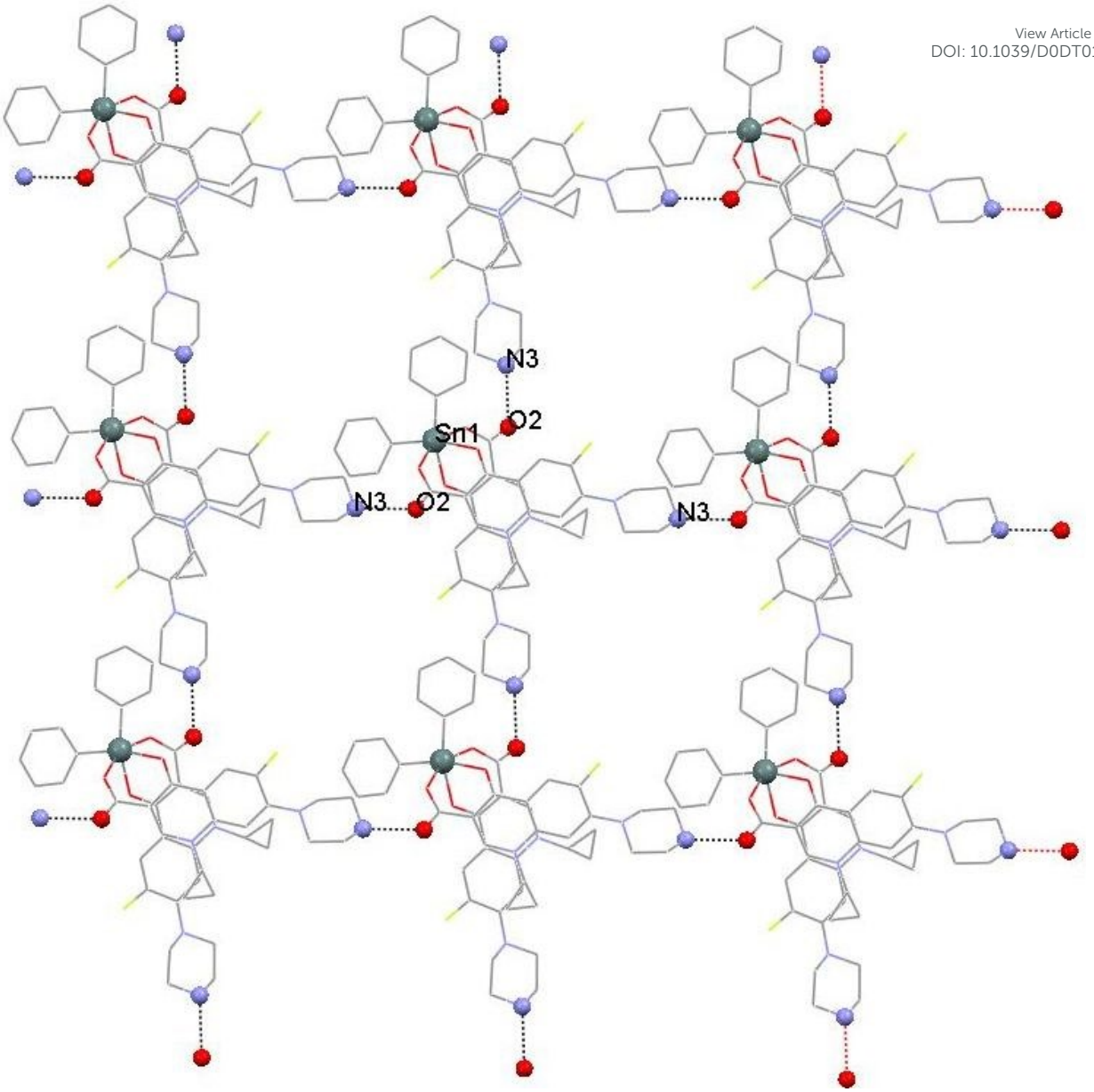

Figure 3

View Article Online
DOI: 10.1039/D0DT01665A

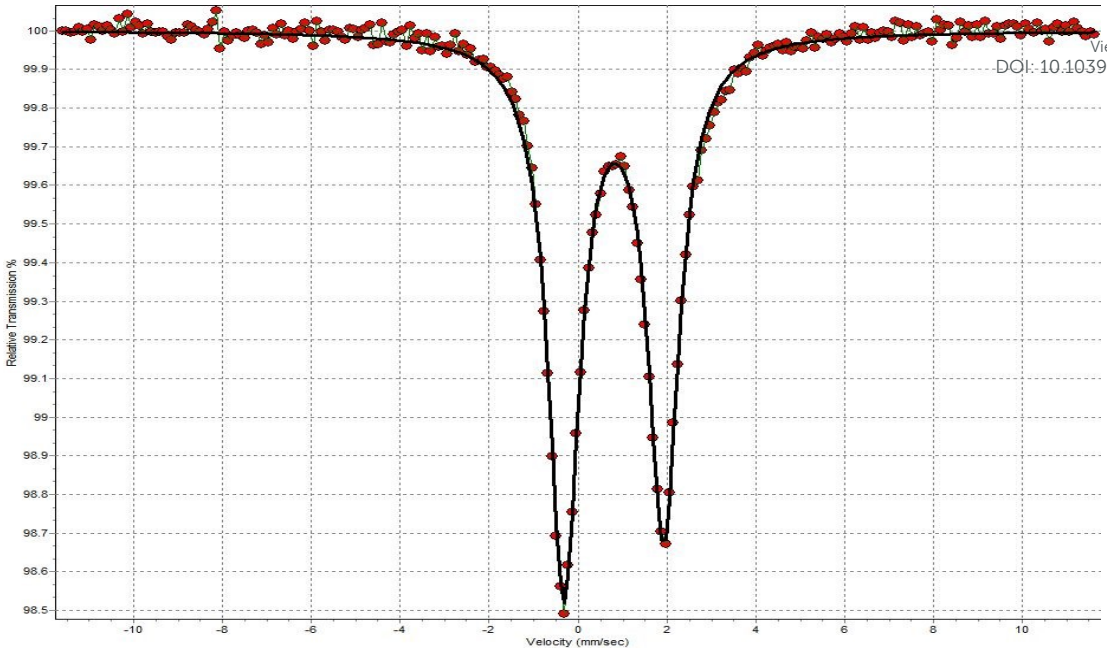

Figure 4

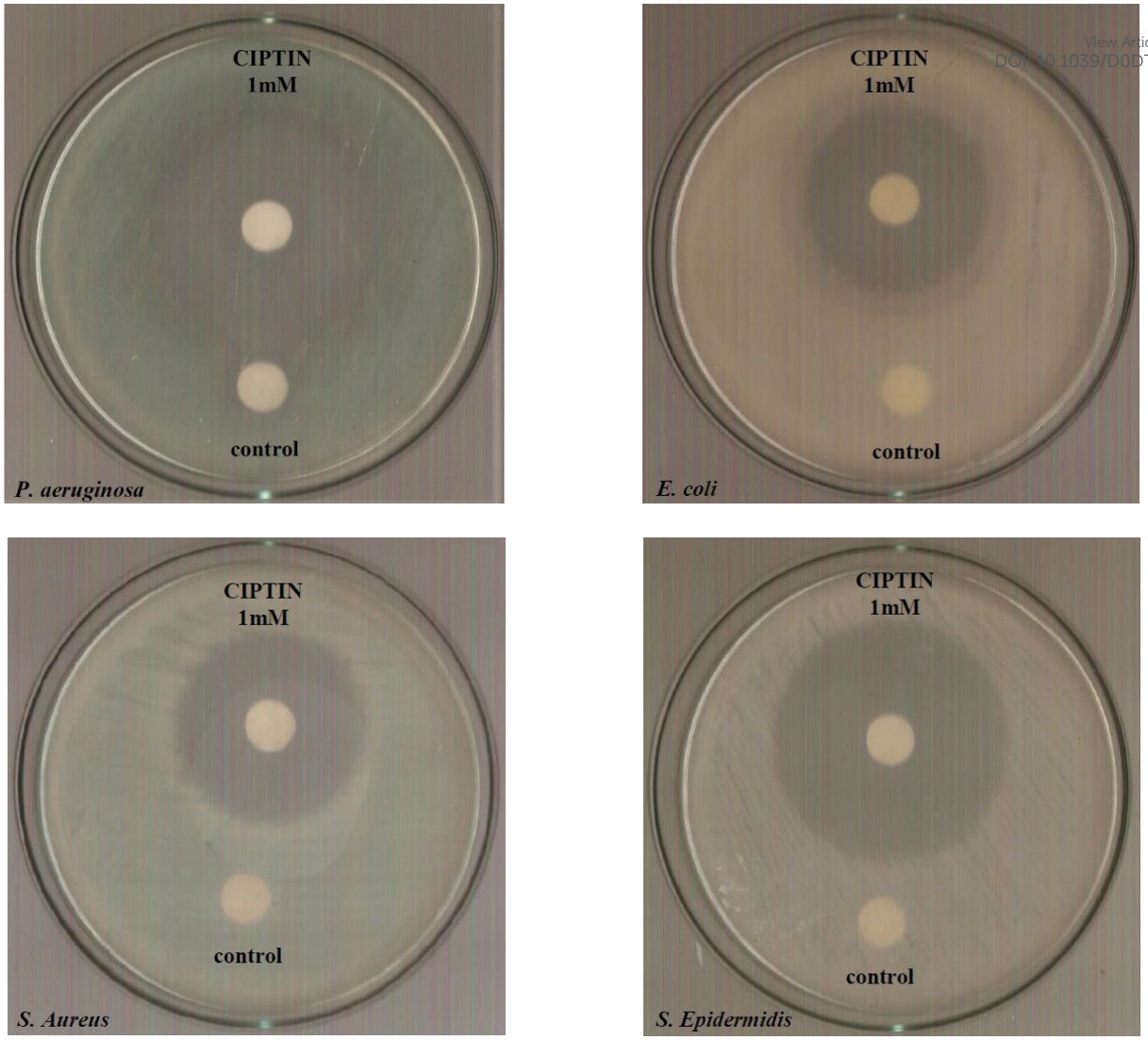

Figure 5

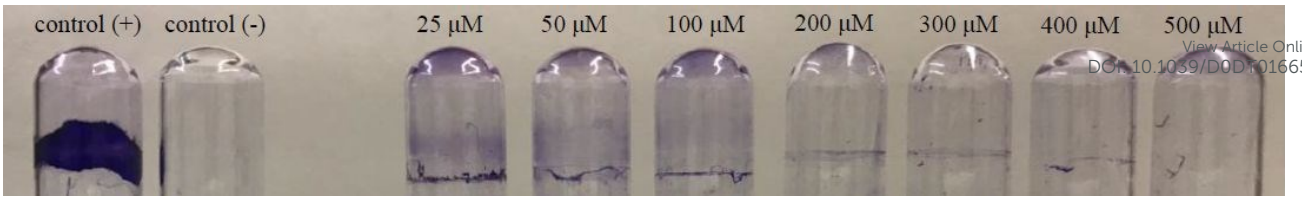

(A)

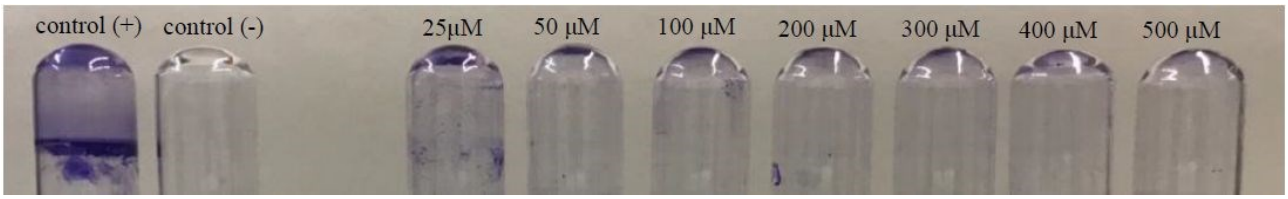

(B)

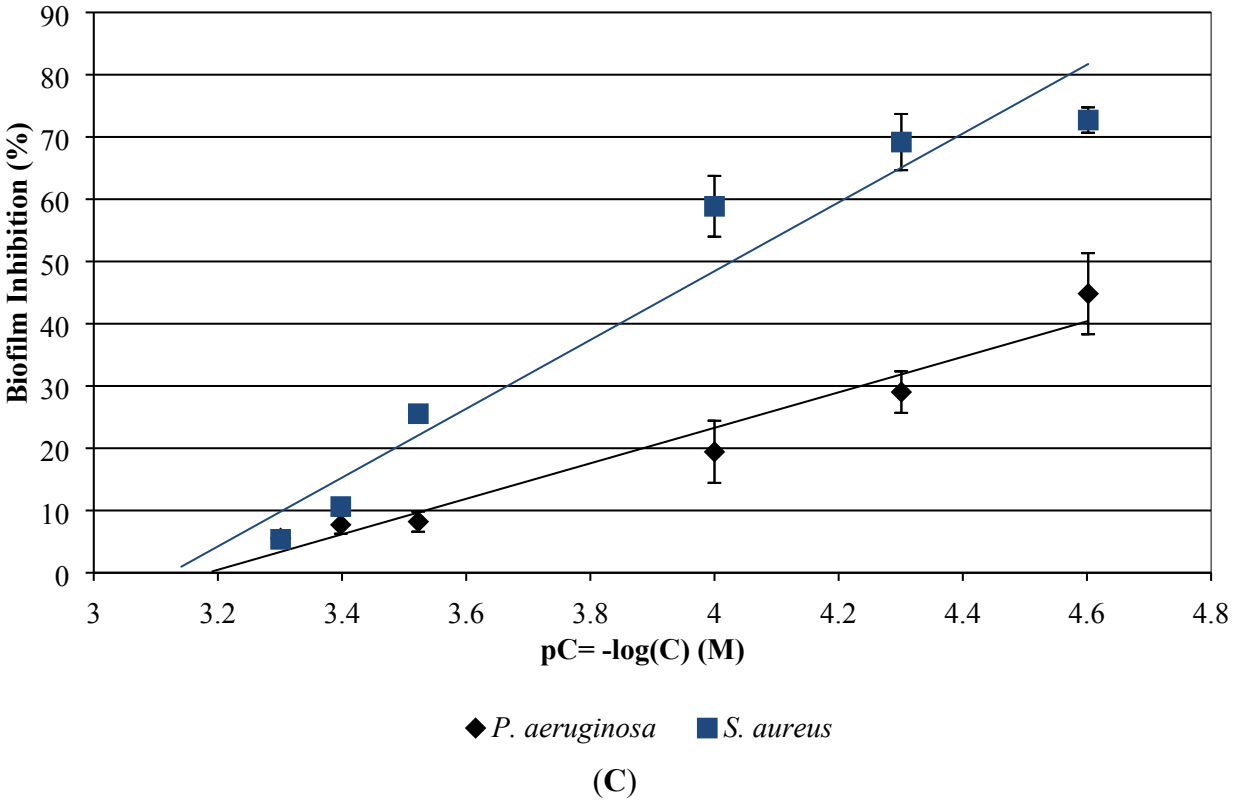

(C)

Figure 6

View Article Online
DOI: 10.1039/D0DT01665A

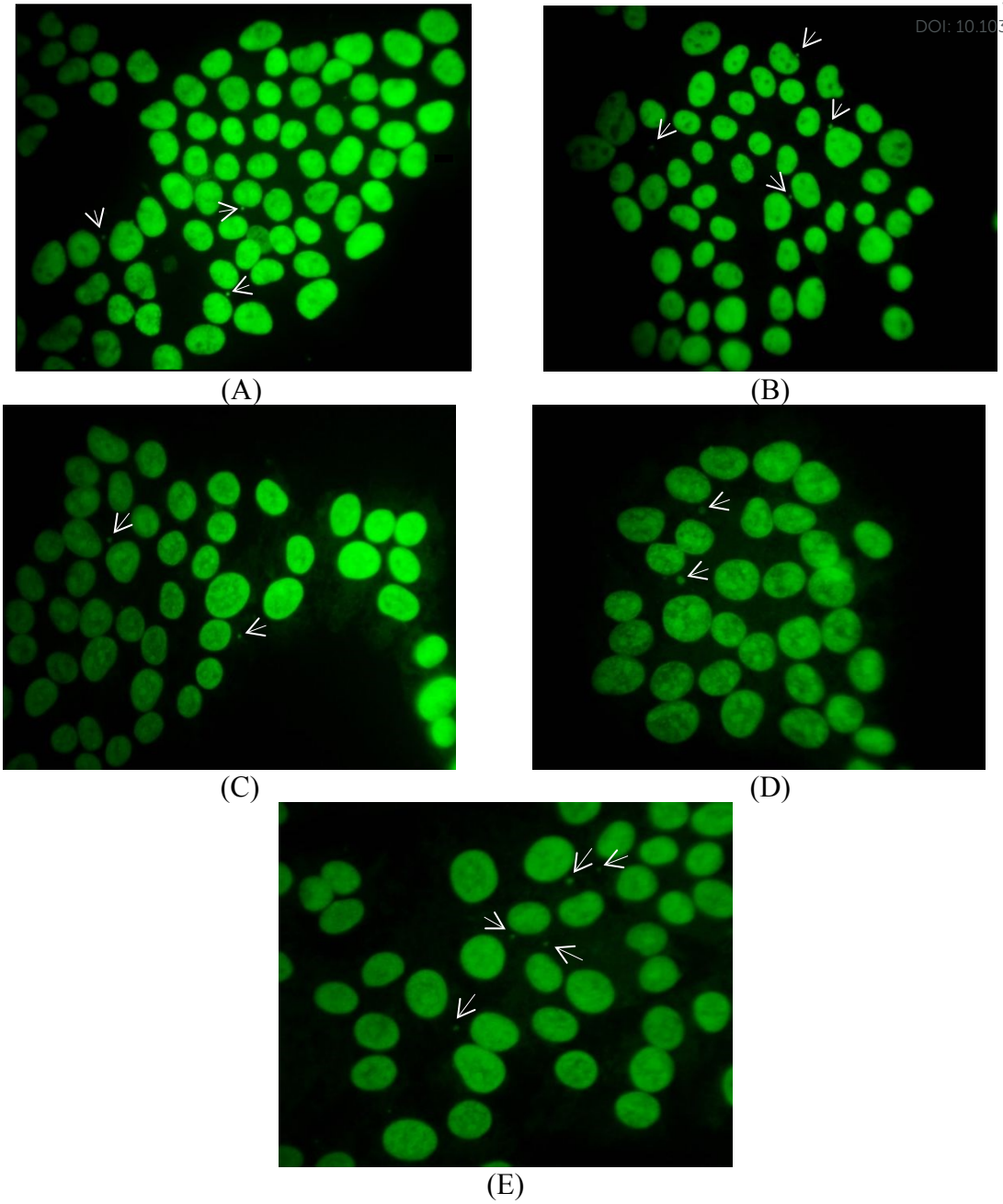

Figure 7

View Article Online
DOI: 10.1039/D0DT01665A

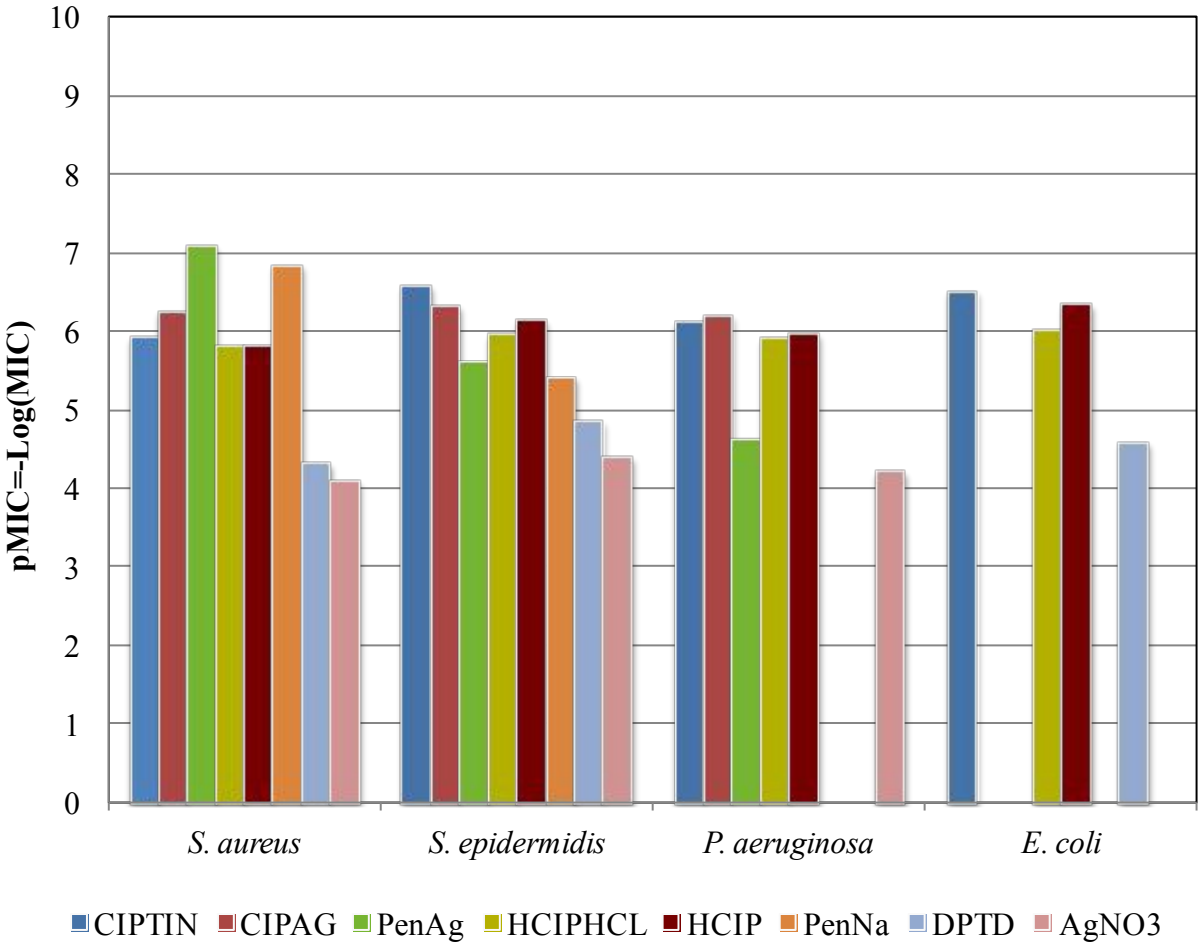

Figure 8

Graphical Abstract

View Article Online
DOI: 10.1039/D0DT01665A

Ciprofloxacin conjugated to diphenyltin(IV); A novel formulation with enhanced antimicrobial activity.

M.P. Chrysouli, C.N. Banti, N. Kourkoumelis, E.E.Moushi, A.J. Tasiopoulos, A. Douvalis, C. Papachristodoulou, A.G. Hatzidimitriou, T. Bakas, S.K. Hadjikakou

The steroisomer Δ-*cis*-[$Ph_2Sn(CIP)_2$] (**CIPTIN)** was obtained from ciprofloxacin and DPTC. **CIPTIN** exhibits stronger activity than ciprofloxacin against Gram positive or negative bacteria